Unconditionally Stable Explicit Schemes for the Approximation of Conservation Laws

Christiane Helzel and Gerald Warnecke

Institut für Analysis und Numerik, Otto-von-Guericke Universität Magdeburg, 39016 Magdeburg, Germany

Abstract. We consider explicit schemes for homogeneous conservation laws which satisfy the geometric Courant-Friedrichs-Lewy condition in order to guarantee stability but allow a time step with CFL-number larger than one. A brief overview over existing unconditionally stable schemes for hyperbolic conservation laws is provided, although the focus is on LeVeque's large time step Godunov scheme. For this scheme we explore the question of entropy consistency for the approximation of one-dimensional scalar conservation laws with convex flux function and describe a possible way to extend the scheme to the two-dimensional case. Numerical calculations and analytical results show that an increase of accuracy can be obtained because the error introduced by the modified evolution step of the large time step Godunov scheme may be less important than the error due to the projection step.

1 Introduction

The long time unsteady numerical dynamics for hyperbolic conservation laws still presents quite a challenge. Most of the published work in this field deals with either steady flows, i.e. the actual limit of infinite time, or rather short time unsteady flow. The basic problem is that hyperbolic conservation laws have solutions with no dissipation in smooth regions and very little nonlinear dissipation at shocks. Numerical approximation always leads to the introduction of dissipation, which is especially strong at shocks. The numerical propagation of waves may also be distorted by a phase error, see Morton [30] for a recent discussion.

Even one-dimensional problems may provide a challenge to modern high-resolution schemes, when numerical results for long time dynamics are required. Examples of such practical applications are long pneumatic or hydraulic pipes in which piston driven pressure waves move back and forth over relatively large distances interacting with each other. Due to the accumulation of the numerical dissipation and phase error, currently available schemes produce useless results for the longer time periods that have to be considered, see Iben and Tadmor [14].

Other numerical problems arise if very different scales are modeled by the equations, for instance in low Mach number flow calculations. In [15], Klein uses the unconditionally stable Godunov-type scheme of LeVeque, which is reviewed in this paper, to calculate the influence of the fast acoustic waves in such a system.

Finite volume schemes are currently the most widely used basic tool for computational fluid dynamics of compressible flows and multidimenensional schemes for hyperbolic conservation laws in general. The idea of solving Riemann problems was introduced by Godunov [6] and was developed considerably in the last two decades. The available number of variants of this numerical approach is quite large and there are many special techniques with corresponding theoretical basis for various applications.

For long time numerics all possibilities for more efficiency of the calculations have to be exploited. This includes adaptive methods, special solvers and any means of increasing the time steps used without sacrificing accuracy. That is where the large time step method of LeVeque, that will be explained in detail below, is of special interest. It provides a simple means of taking larger time steps for one-dimensional systems with Riemann solver based finite volume schemes.

In Section 2 we provide the basic theoretical and numerical concepts of conservation laws which are used in this paper. A short overview over existing unconditionally stable schemes for conservation laws is given in Section 3 followed by a detailed review of the large time step Godunov-type scheme of LeVeque in Section 4. In order to get an entropy-consistent solution for problems which contain rarefaction waves, it is necessary to use an entropy consistent Riemann solver in every time step. Such Riemann solvers are discussed in some detail. Nevertheless, the question whether the large time step Godunov scheme gives an entropy consistent approximation for 1D nonlinear systems of conservation laws is still unsolved. For the case of scalar conservation laws with convex flux function new results could be obtained, which are discussed in Section 5. An extension of the large time step method for two space dimensions is discussed in Section 6.

2 Basic concepts for the numerical approximation of conservation laws

2.1 Hyperbolic conservation laws

We consider numerical schemes for solving nonlinear *hyperbolic systems of conservation laws*, i.e. equations of the general form

$$\frac{\partial}{\partial t}\mathbf{u} + \sum_{i=1}^{d} \frac{\partial}{\partial x_i}\mathbf{f}_i(\mathbf{u}) = \mathbf{0} \tag{1}$$

with given initial values

$$\mathbf{u}(\mathbf{x},0) = \mathbf{u}_0(\mathbf{x}) \tag{2}$$

where $\mathbf{x} \in \mathbb{R}^d$, $t \in \mathbb{R}^+ = \{t \in \mathbb{R} : t \geq 0\}$ and $\mathbf{u} : \mathbb{R}^d \times \mathbb{R}^+ \to \mathbb{R}^p$ is a vector valued function of conserved quantities, e.g. mass, momentum, and energy for the Euler equations. The vector valued functions $\mathbf{f}_i : \mathbb{R}^p \to \mathbb{R}^p$ are called flux functions.

The physical interpretation of this system of equations can be seen by rewriting (1) into the following *integral form* by using the Gauss theorem

$$\frac{\partial}{\partial t}\int_{\Omega} \mathbf{u} d\mathbf{x} + \sum_{i=1}^{d} \int_{\partial\Omega} \mathbf{f}_i(\mathbf{u}) n_i dS = \mathbf{0}, \tag{3}$$

where Ω is an arbitrary domain of $\mathbb{R}^d$ and $\mathbf{n} = (n_1, \ldots, n_d)^T$ is the outward unit normal vector of the boundary $\partial\Omega$ of the considered domain Ω. Now the change of the total amount in Ω of the conserved quantities given by $\int_{\Omega} \mathbf{u} d\mathbf{x}$ is equal to the outward flux through the surface $\partial\Omega$.

Another form, the *quasilinear form*, of (1) can be obtained by carrying out the differentiations of the flux functions, then we get

$$\frac{\partial}{\partial t}\mathbf{u} + \sum_{i=1}^{d} \mathbf{A}_i(\mathbf{u}) \frac{\partial}{\partial x_i}\mathbf{u} = \mathbf{0} \tag{4}$$

where $\mathbf{A}_i(\mathbf{u}) = \mathbf{f}'(\mathbf{u})$ is the Jacobian matrix of the flux function $\mathbf{f}_i$. The d-dimensional system of conservation laws is called *hyperbolic*, if for any $\mathbf{u} \in \Omega$ and any $\mathbf{w} \in \mathbb{R}^d$, $\mathbf{w} \neq \mathbf{0}$ the matrix $\sum_{i=1}^{d} w_i \mathbf{A}_i(\mathbf{u})$ has p real eigenvalues $\lambda_1(\mathbf{u}) \leq \ldots \leq \lambda_p(\mathbf{u})$ and a complete set of linearly independent right eigenvectors $\mathbf{r}_1(\mathbf{u}), \ldots, \mathbf{r}_p(\mathbf{u})$.

Nice descriptions of the theory of hyperbolic conservation laws as well as the concepts of numerical schemes can be found in the text books of Godlewski, Raviart [4], [5], Kröner [16] and LeVeque [26], [28]. Here we briefly want to cover those definitions and theoretical results which will be needed for our considerations.

The solution to the initial value problem (1), (2) is in general not continuous, i.e. the solution may contain shocks. Therefore we are not only interested in classical, i.e. differentiable solutions of (1), (2) but also in *weak* solutions which allow discontinuities. Though one could develop the integral form (3) into a definition of weak solutions we prefer to use the distributional form.

Definition 1. Assume that the initial values $\mathbf{u}_0$ are in the space of locally bounded measurable functions, i.e. $\mathbf{u}_0 \in L^{\infty}_{loc}(\mathbb{R}^d)^p$. A function $\mathbf{u} \in L^{\infty}_{loc}(\mathbb{R}^d \times \mathbb{R}^+)^p$ is called a *weak solution* of the Cauchy problem (1), (2) if $\mathbf{u}$ satisfies the integral equation

$$\int_0^{\infty}\int_{\mathbb{R}^d} \left(\mathbf{u}\frac{\partial}{\partial t}\varphi + \sum_{i=1}^{d} \mathbf{f}_i(\mathbf{u})\frac{\partial}{\partial x_i}\varphi \right) d\mathbf{x}dt + \int_{\mathbb{R}^d} \mathbf{u}_0(\mathbf{x})\varphi(\mathbf{x}, 0) d\mathbf{x} = \mathbf{0} \tag{5}$$

for all test functions $\varphi \in C_0^{\infty}(\mathbb{R}^d, \mathbb{R}^+)^p$, i.e. vector valued test functions of compact support in $\mathbb{R}^d \times \mathbb{R}^+$ which are infinitely smooth.

Equation (5) implies that jump discontinuities in weak solutions are not completely arbitrary. At a point of discontinuity the two states $\mathbf{u}_+$, $\mathbf{u}_-$ between which the solution jumps are related to the geometry of the surface of discontinuity by the *Rankine-Hugoniot condition.* It says that the relation

$$[\mathbf{u}_+ - \mathbf{u}_-]n_t + \sum_{j=1}^{d} [\mathbf{f}_j(\mathbf{u}_+) - \mathbf{f}_j(\mathbf{u}_-)]\, n_{x_j} = \mathbf{0} \tag{6}$$

has to hold, where the vector $\mathbf{n} = (n_t, n_{x_1}, \dots, n_{x_d})$ is the normal of the surface of discontinuity.

Even if weak solutions with a jump discontinuity satisfy the Rankine-Hugoniot condition they are not necessarily unique. We need an additional condition to characterize the physically relevant weak solutions, which is called an *entropy condition.* There is no general theory for multidimensional systems available. For scalar conservation laws and systems in one space dimension a number of mathematical criteria such as the Lax condition, various entropy inequalities or the viscosity method are in use, see [4], [5], [26], [34].

For a given numerical scheme we do not only have to know whether the sequence of approximate solutions is convergent. We also have to consider whether the limit solution is actually the physically relevant solution to the problem considered. In order to show this entropy consistency of a given numerical scheme at least for scalar conservation laws, various equivalent entropy conditions can be applied, see [26]. We will consider the question of entropy consistency for the large time step Godunov scheme of LeVeque[22] in Section 5.

2.2 Numerical schemes for conservation laws

A general framework for many numerical schemes for solving systems of conservation laws with given initial values and boundary conditions consists of the following steps: A *projection* of the initial values respectively of the numerical solution at the previous time step onto piecewise constant step functions corresponding to the underlying mesh. This is followed by an *evolution step* in which the system of conservation laws with initial values corresponding to this finite dimensional subspace of step functions is solved either exactly or numerically. The evolution step can be carried out in many different ways, leading to different numerical schemes. We will restrict our considerations to Godunov-type schemes, which were introduced by Godunov [6], where the evolution is calculated by solving Riemann problems between neighboring mesh cells. Higher-resolution can be obtained by considering the evolution of piecewise linear instead of piece constant functions.

Now we first want to restrict our considerations to the case of one space dimension, i.e. we are looking for a numerical solution of the system of conservation laws

$$\mathbf{u}_t(x,t) + \mathbf{f}_x(\mathbf{u}(x,t)) = 0,$$

with given initial values $\mathbf{u}(x,0)$, where $\mathbf{u}$ and $\mathbf{f}$ are in $\mathbb{R}^p$. The numerical calculations have to be restricted to a bounded interval $[a,b] \in \mathbb{R}$ with appropriate numerical boundary conditions.

For a given discretization $a = x_{-\frac{1}{2}} < x_{1+\frac{1}{2}} < \ldots < x_{m+\frac{1}{2}} = b$ of the computational interval $[a,b]$ at time t_n, we can define a piecewise constant vector valued function $\mathbf{u}^n(x,t_n) = \mathbf{U}_i^n(x)$ for $x \in [x_{i-\frac{1}{2}}, x_{i+\frac{1}{2}})$, where

$$\mathbf{U}_i^n = \frac{1}{h}\int_{x_{i-\frac{1}{2}}}^{x_{i+\frac{1}{2}}} \mathbf{u}(x,t_n)dx$$

is the cell average of the exact or numerical solution $\mathbf{u}$ in the mesh cell $[x_{i-\frac{1}{2}}, x_{i+\frac{1}{2}})$ at time t_n. We will always use k to denote the time step and h to describe the mesh width of a one-dimensional scheme. The solution at the next time step can now be calculated by solving Riemann problems at each cell interface, i.e. solving the conservation law with initial values consisting of two constant states. We get these Riemann problems by considering the cell averages between two neighboring mesh cells. The solution of the Riemann problem consist in general of constant states which are connected by shocks, rarefaction waves or contact discontinuities, see Smoller [34].

For some conservation laws, for instance the Euler equations of gas dynamics, the Riemann problem can be solved exactly. See Chorin [2] for a scheme where the exact Riemann solution is approximated. For many applications it is not necessary or possible to get an exact solution of the Riemann problem. Therefore approximative Riemann solvers were developed. One which is often used is the Roe solver, see [31] or any text book on numerical schemes for conservation laws [5], [26], [35]. The use of the Roe Riemann solver for an unconditionally stable extension of a Godunov-type scheme is considered in Section 4.1.

As long as the waves coming from neighboring Riemann problems do not interact as shown in Figure 1 (a), we can calculate the solution $\mathbf{u}(x,t)$ for $t > t_n$ at every point x. This solution can be written in the form

$$\mathbf{u}(x,t) = \mathbf{u}^n(x,t_n) + \sum_j \left(\mathbf{u}_j^n(x,t) - \mathbf{u}_j^n(x,t_n)\right) \tag{7}$$

where

$$\mathbf{u}_j^n(x,t_n) = \begin{cases} \mathbf{U}_{j-1}^n & : x < x_{j-\frac{1}{2}} \\ \mathbf{U}_j^n & : x \geq x_{j-\frac{1}{2}} \end{cases} \tag{8}$$

is a piecewise constant function, defined over the whole x axis as the Riemann initial values corresponding to the jump across the cell interface at $x_{j-\frac{1}{2}}$. The solution $\mathbf{u}(x,t)$ calculated via (7) consists of the piecewise constant solution $\mathbf{u}^n(x,t_n)$ at the previous time step plus possibly a wave in $\mathbf{u}$ due to a Riemann problem with an influence at the point x. Here $\mathbf{u}_j^n(x,t)$ is the numerical or exact Riemann solution at a point x and time t to the initial values $\mathbf{u}_j^n(x,t_n)$. As long as there are no interactions between the waves of neighboring Riemann problems there is always at most one Riemann problem that modifies the solution $\mathbf{u}(x,t)$ at a fixed position x and time t. Therefore, we can calculate the solution $\mathbf{u}(x,t)$ at every point x by only solving Riemann problems. This classical version of a Godunov-type scheme requires a time step restriction so that the fastest wave occurring by considering all Riemann problems at a given time t_n can only move through a half mesh cell during one time step. This is guaranteed by requiring

$$CFL := \max_i \max_w |\lambda_w(\mathbf{u}_{i-1}, \mathbf{u}_i)| \frac{k}{h} \leq \frac{1}{2},$$

where $\lambda_w(\mathbf{u}_{i-1}, \mathbf{u}_i)$ is the w-th eigenvalue of the Jacobian matrix of the flux function at the cell interface between the mesh cells $i-1$ and i. This is a special and, as we see below, more restrictive than necessary form of the *Courant-Friedrich-Lewy (CFL) condition*, which was introduced in [3]. In general the CFL condition says, see [3], that a *necessary* condition for a numerical scheme to be stable and therefore convergent is that its numerical domain of dependence contains the true domain of dependence of the partial differential equation considered, at least in the limit as k and h go to zero.

For a linear system $\mathbf{u}_t + \mathbf{A}\mathbf{u}_x = \mathbf{0}$ with $\mathbf{A} \in \mathbb{R}^{m \times m}$ the domain of dependence of the exact solution at a given point (x,t) consists of the m points $x - \lambda_1 t, \ldots, x - \lambda_m t$. If we use a numerical scheme where the solution in one mesh cell is only influenced by the neighboring mesh cells as it is the case for the Godunov scheme, then we have to require that the exact domain of dependence has to be inside this numerical domain of dependence. For a linear system this gives us the time step restriction $|\lambda_{max}| \frac{k}{h} \leq 1$.

The wave speeds s_w arising in the Riemann problem for a linear system are equal to the eigenvalues λ_w of the matrix $\mathbf{A}$. For a nonlinear system of conservation laws the maximal eigenvalues are a upper bound of the maximal occurring wave speeds. This gives us a time step restriction $CFL \leq 1$, where now waves from neighboring Riemann problems might interact with each other. That the interaction of waves inside one mesh cell does not lead to serious problems, even if we consider nonlinear systems of equations, is due to the fact that we are only interested in the cell averages of the solution $\mathbf{U}_i^{n+1}$ for every mesh cell. This is because only the cell averages are needed as initial values for the next time step. In order to calculate the cell averages it is not necessary to calculate the solution $\mathbf{u}(x,t)$ for every point $x \in [x_{i-\frac{1}{2}}, x_{i+\frac{1}{2}})$. Instead we only need to calculate the flux through the boundaries at each mesh cell. This can be seen by considering the following integral form of the conservation law for every mesh cell, see LeVeque [26]

$$\int_{x_{i-\frac{1}{2}}}^{x_{i+\frac{1}{2}}} \mathbf{u}(x,t_{n+1})dx = \int_{x_{i-\frac{1}{2}}}^{x_{i+\frac{1}{2}}} \mathbf{u}^n(x,t_n)dx + \int_{t_n}^{t_{n+1}} \Big(\mathbf{f}(\mathbf{u}^n(x_{i-\frac{1}{2}},t)) - \mathbf{f}(\mathbf{u}^n(x_{i+\frac{1}{2}},t))\Big)\, dt.$$

This is equivalent to the *conservative form* of the Godunov scheme

$$\mathbf{U}_i^{n+1} = \mathbf{U}_i^n - \frac{k}{h}\left(\mathbf{F}_{i+\frac{1}{2}}(\mathbf{U}_i^n, \mathbf{U}_{i+1}^n) - \mathbf{F}_{i-\frac{1}{2}}(\mathbf{U}_{i-1}^n, \mathbf{U}_i^n)\right),$$

with the *numerical flux function*

$$\mathbf{F}_{i+\frac{1}{2}}(\mathbf{U}_i^n, \mathbf{U}_{i+1}^n) = \frac{1}{k}\int_{t_n}^{t_{n+1}} \mathbf{f}(\mathbf{u}^n(x_{i+\frac{1}{2}}, t))dt.$$

Therefore, we only have to determine the flux along the cell boundaries. This is relatively easy because the solution is constant at the cell boundary as long as no wave from a neighboring Riemann problem crosses the cell interface. This again shows that the time step restriction shown in Figure 1 (a), where the fastest wave can maximally move through half of the neighboring mesh cell, is more restrictive then necessary. The flux difference form of the Godunov scheme allows time steps where the fastest wave can maximally go through one mesh cell as indicated in Figure 1 (b).

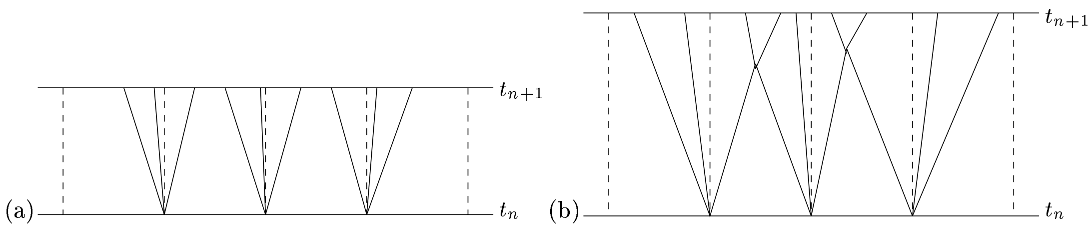

Fig. 1. Waves arising in the solution of Riemann problems for one time step of the Godunov scheme; left: $CFL \leq 0.5$, right: $CFL \leq 1$

After having defined the basic concept of the Godunov scheme we now want to review some analytical properties. For the Godunov scheme, one has a consistency result which says that if in the limit, when k and h go to zero, the scheme is convergent, then the limit function is a weak solution. This is a consequence of the Lax-Wendroff Theorem [17], which more generally holds for schemes which can be written in conservative form so that the numerical flux function is consistent with the flux function of the conservation law, i.e. $\mathbf{F}(\mathbf{u}, \mathbf{u}) = \mathbf{f}(\mathbf{u})$.

In the general form, the Lax-Wendroff Theorem does not say whether the Godunov scheme, or any conservative scheme, converges at all. Indeed, it is possible to construct conservative and consistent schemes which are unstable and therefore of no use. On the other hand, even if the scheme converges, the weak solution is not unique in general which leads to the question whether the Godunov scheme is *entropy consistent*, i.e., whether the limit solution is the physical relevant solution of the problem considered. For the Godunov scheme we get a positive answer to the latter question from the Harten-Lax Theorem, see [10], [11]. There the discrete form of the entropy inequality, a special form of the entropy condition, is used to pick out the physical relevant weak solution.

The concept of the Godunov scheme is implemented in the software package CLAWPACK [18], which was used for our calculations. It may be used with any Riemann solver. There the wave propagation algorithm developed by LeVeque [27] is used to update the solution $\mathbf{u}$ at every time step. High-resolution can be obtained by considering piecewise linear reconstruction. This requires the use of limiter functions in order to avoid spurious oscillations along shock fronts, see [27]. The CLAWPACK program considers very general problems, including conservation laws with a capacity function or conservation laws with source terms in one, two, and three dimensions, see [19], [27] or [28] for details.

The simplest way to extend a one dimensional method to a multidimensional scheme is to use a *dimension splitting* approach. For a two-dimensional problem one could for instance first apply the Godunov scheme in x direction to calculate new cell averages which are then used as initial values for applying the Godunov scheme in y direction. These splitting schemes perform well for many test cases, but the solution might depend on the mesh which was used for the calculation because the mesh determines the preferred direction which is approximated by the scheme. Other schemes, for instance the finite volume scheme in CLAWPACK, were developed in order to approximate more closely the multidimensional behavior of the equations, see [27].

3 Unconditionally stable schemes for conservation laws

In contrast to the situation for numerical methods discretizing ordinary differential equations, it is possible to derive unconditionally stable explicit schemes, i.e., explicit schemes without a restriction of the time step, for the approximation of conservation laws. That this is possible, in principle, can be seen by considering the geometric CFL condition, i.e. that the domain of dependence of the exact solution must be contained in the domain of dependence for the numerical solution. This necessary condition for stability is satisfied if the space stencil of the scheme is automatically increased with a larger time step.

A generalization of the Godunov scheme which allows larger time steps was developed by LeVeque, see [20], [22]. In the following we will refer to this scheme as the LTS Godunov-type scheme. Here the interaction of waves corresponding to neighboring Riemann problems is approximated as a linear superposition. We will review this approach in the next section.

A generalization of the Glimm scheme to an unconditionally stable scheme was considered by Wang in [37]. In difference to the LTS Godunov-type scheme the piecewise constant initial values for the next time step are obtained by taking the exact or approximative solution at some randomly chosen point in the mesh cell instead of the cell average over the solution which is use by Godunov type schemes.

An unconditionally stable scheme based on Front tracking was developed by Holden and Risebro [13]. The good performance of this scheme for the Euler equations is demonstrated in [12].

Billett and Toro [1] consider the weighted average flux (WAF) scheme which allows time steps with Courant numbers up to two, see [36].

Finally, we note that unconditionally stable explicit methods, based on rational Runge-Kutta methods, have been considered for parabolic equations in the past, see Hairer [7] and Satofuka [32]. They were also used in flow calculations, see Satofuka [33].

4 The large time step Godunov scheme of LeVeque

Now we want to consider the LTS Godunov scheme of LeVeque [20], [21], [22], [25] applied to one dimensional systems of conservation laws. As we have seen in Section 2.2 the classical concept of the Godunov scheme, where the solution $\mathbf{u}$ is defined as the combination of the solution of Riemann problems as long as there are no interactions of waves, can be extended to the case $CFL \leq 1$ in which no wave can cross a neighboring cell interface. In order to extend the Godunov scheme to time steps with $CFL > 1$, one also has to take the interaction of waves into consideration. In the LTS Godunov scheme this interaction is approximated by linear superposition of waves, which means that the interaction of waves will not lead to a change of the speed or strength of the waves, as indicated in Figure 2. In the nonlinear case the waves would have an influence on each other which would lead to a change of the wave speed, direction and strength as shown in Figure 1 (b).

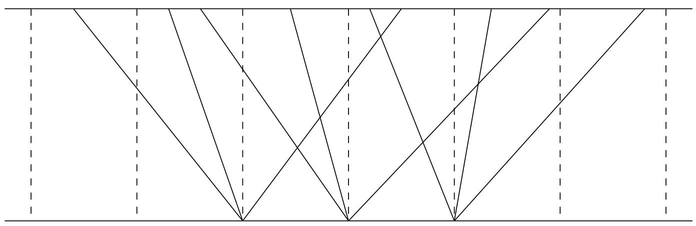

Fig. 2. Linear interaction of waves as approximated by the large time step Godunov scheme

The LTS Godunov scheme can also be defined via equation (7) with the only difference that for a given point x there may be not only one Riemann problem that leads to a change of $\mathbf{u}(x,t)$. The numerical solution $\mathbf{u}(x,t)$ at a given point x is equal to the value $\mathbf{u}(x, t_n)$ at the old time step plus the jump in $\mathbf{u}$ across all waves which have crossed the line between (x, t_n) and (x, t), see [22].

In [21], LeVeque has proved that his modification of the Godunov scheme, with an appropriate Riemann solver for each Riemann problem occurring in the discretization as it will be discussed in Section 4.1, can be written in conservative form with a numerical flux function that is consistent with the conservation law. Hence, if the scheme converges in the limit as k and h go to zero, the limit function is a weak solution, in consequence of the Lax-Wendroff Theorem.

For scalar conservation laws he could also show that the approximate solution is total variation diminishing for arbitrary Courant numbers. This property implies via Helly's Theorem that for every subsequence of the mesh discretization, with $k_l \to 0$ and $k_l/h_l = const$, every sequence of approximate solutions contains a convergent subsequence locally in L^1. Together with the Lax-Wendroff Theorem this gives convergence of the LTS Godunov scheme to a weak solution at least in the case of scalar conservation laws.

Furthermore, he conjectured that the approximated weak solution is consistent with the entropy condition, i.e. is the physical relevant weak solution of the scalar conservation law. The proof of the entropy consistency turned out to be difficult due to the fact that the scheme is not monotone. Some preliminary results concerning the entropy consistency of the LTS Godunov scheme and the LTS Glimm scheme where shown in Wang, Warnecke [38], [39].

4.1 The solution of the Riemann problem

A necessary condition in order to get an entropy stable approximation is that the solution $\mathbf{u}_j^n(x, t)$ of each single Riemann problem is entropy consistent. This can always be obtained by using an exact Riemann solver. Since we are only interested in the cell averages of the numerical solution at discrete time steps, the use of entropy consistent approximative Riemann solvers is often easier and leads to the same accuracy of the numerical results.

Here we want to consider the use of Roe's Riemann solver, see [31], for the LTS scheme. Roe suggested instead of determining the Riemann solution of a given nonlinear system to calculate the solution of the Riemann problem for a corresponding *linear system*

$$\mathbf{u}_t + \mathbf{A}(\mathbf{u}_L, \mathbf{u}_R)\mathbf{u}_x = \mathbf{0}, \quad \mathbf{u}(x, 0) = \begin{cases} \mathbf{u}_L : x < x_0 \\ \mathbf{u}_R : x \geq x_0 \end{cases}$$

where the matrix $\mathbf{A}(\mathbf{u}_L, \mathbf{u}_R)$ has to be a consistent approximation of the Jacobian matrix for the Riemann problem. Furthermore, the Rankine-Hugoniot condition has to be satisfied and finally the constant matrix $\mathbf{A}(\mathbf{u}_L, \mathbf{u}_R)$ has to be diagonalizable with real eigenvalues, see for instance [26]. This means that the solution of the Riemann problem for a nonlinear system of conservation laws is reduced to the solution of the Riemann problem for a linear system, which displays locally the basic properties of the nonlinear system.

The Riemann problem for the resulting linear system can be solved exactly. A disadvantage of this approach comes from the fact that the solution of a linear system only consists of discontinuities, whereas the Riemann solution of a nonlinear hyperbolic conservation law can also contain rarefaction waves. Fortunately, in most situations this does not lead to any problems because the change in the cell average of the solution caused by a rarefaction wave can usually be approximated by a single discontinuity moving with a speed that is equal to the average between the most left and the most right going part of the rarefaction wave. The only situation in which the Roe solver fails for $CFL \leq 1$ is the case of a rarefaction wave with $\lambda(\mathbf{u}_L) < 0 < \lambda(\mathbf{u}_R)$ for one eigenvalue of the Jacobian matrix, e.g. as in transonic flows. The approximation of a rarefaction wave by a discontinuity has the effect that either the cell average at the left hand side or the cell average at the right hand side will be influenced. In the case of a transonic rarefaction wave both cell averages should be changed. An entropy-fix has to be used to overcome this problem, see for instance Harten and Hyman [8].

For the LTS scheme the entropy-fix has to be extended. In order to explain this, we want to consider the approximation of a rarefaction wave for a scalar conservation law, for instance the Burgers equation. It can be extended to systems of conservation laws in an analogous way with the only difference that the solution of the Riemann problem consists of more than one wave.

If the exact solution of the Riemann problem is a *shock*, then we can calculate the shock speed using the Rankine-Hugoniot condition. The jump across the shock is equal to the jump of the Riemann initial values. This jump is added to all the cell averages of the mesh cells which were crossed by this wave during the time step. The jump is partially added to the cell averages of the mesh cells which were only touched by the wave.

If the solution of the Riemann problem with initial values u_L for $x < x_0$ and u_R for $x \geq x_0$ is a *rarefaction wave*, then in the case of a convex flux function the solution is equal to

$$u(x,t) = \begin{cases} u_L & : \quad (x-x_0)/t < \lambda(u_L) \\ u_L + \frac{(x-x_0)/t - \lambda(u_L)}{\lambda(u_R)-\lambda(u_L)}(u_R - u_L) & : \lambda(u_L) \leq (x-x_0)/t < \lambda(u_R) \\ u_R & : \quad (x-x_0)/t \geq \lambda(u_R) \end{cases}$$

Our numerical discretization of a rarefaction wave consists of a piecewise constant step function as shown in the middle of Figure 3. The most left and the most right going parts are the solid lines in Figure 3. If the rarefaction wave at the new time step is spread out over more than one mesh cell, then we introduce new waves, shown as dashed lines in Figure 3, so that there is one jump discontinuity in every mesh cell between $x_0 + \lambda(u_L)\triangle t$ and $x_0 + \lambda(u_R)\triangle t$.

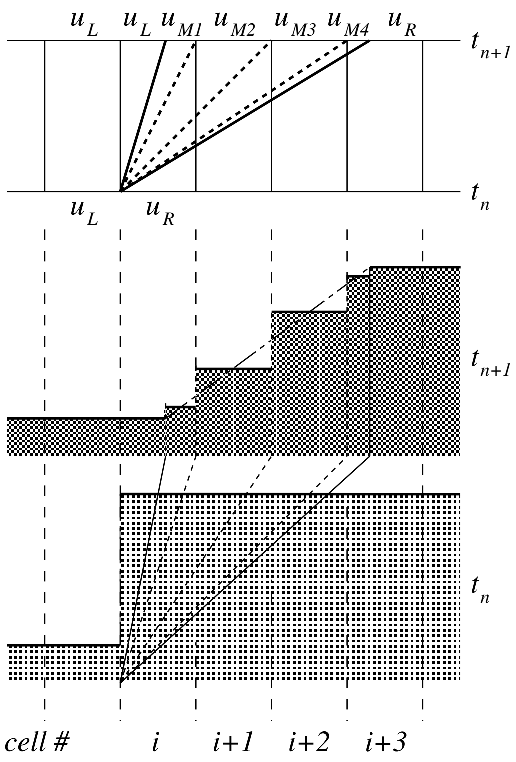

Fig. 3. Approximation of a rarefaction wave that is spread out over different mesh cells

The jumps cross each of these newly introduced waves as well as across the most left and the most right going wave are chosen in such a way that the jump in the initial values is equally distributed to all of these waves. A similar approximation of rarefaction waves was used in LeVeque [23].

4.2 A geometric interpretation of the entropy-fix

In order to approximate the correct cell average for a rarefaction wave, we do not always need to use several waves. In Figure 4 different possibilities for the occurrence of rarefaction waves are shown. The most left and the most right going part of the rarefaction wave are plotted as solid lines. The dashed pointed line in each case corresponds to the speed calculated by the Rankine-Hugoniot condition, i.e. is equivalent to the wave speed used by the Roe solver. The dashed lines are the waves which were introduced to approximate the rarefaction wave.

Considering Figure 4 (a) it becomes clear that if the rarefaction wave at time t_{n+1} is only extended over a single cell then we are able to calculate

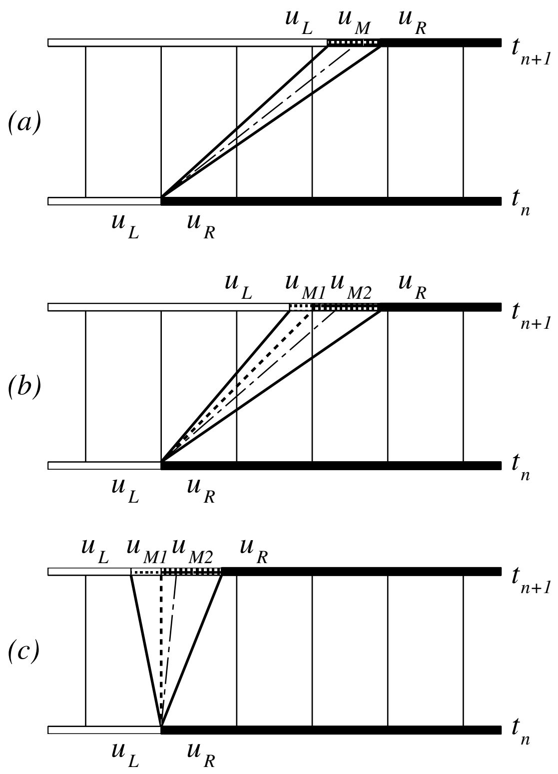

Fig. 4. Geometric interpretation of the entropy-fix for rarefaction waves

the change of the cell average by approximating the rarefaction wave by a single discontinuity which satisfies the Rankine-Hugoniot condition. If the rarefaction wave at time t_{n+1} is spread out over more than one mesh cell, as shown in Figure 4 (b), we need an entropy-fix, i.e. we need to introduce further waves, in order to approximate the correct cell averages.

For the Godunov scheme with Courant number smaller than one, the only possibility of a rarefaction wave that is spread out over more than one mesh cell is shown in Figure 4 (c). Hence the Godunov-type scheme with Roe Riemann solver and $CFL \leq 1$ needs an entropy-fix in the case of a transonic rarefaction wave only.

4.3 The error of the LTS Godunov scheme

There are two components which have an influence on the error of the LTS Godunov scheme. In each time step we make a projection onto piecewise constant functions, which are then used as initial values for the next time step. This leads to a projection error in every time step. By using larger time steps the projection error is reduced because fewer projections in comparison with the classical Godunov-type scheme are necessary in order to calculate the solution at a fixed time.

The second part of the error is generated in the evolution step. The LTS Godunov scheme handles the interaction of waves as a linear superposition which can lead to a large error, especially at discontinuities in nonlinear problems.

The reduction of the projection error can best be seen by considering linear problems, because then the linear superposition of waves is exact and the only error of the scheme is due to the projections in each time step. Here we consider the LTS approximation of a conservation law with capacity function, which is implemented in CLAWPACK, see [19, note # 6].

Example 2. We consider the conservation law with capacity function

$$\kappa(x)u_t + 2u_x = 0, \qquad \kappa(x) = \begin{cases} 2 : x < 5 \\ 1 : x \geq 5 \end{cases}$$

In CLAWPACK solutions for systems of conservation laws with capacity function are calculated using the flux difference form

$$\mathbf{U}_i^{n+1} = \mathbf{U}_i^n - \frac{\triangle t}{\kappa_i \triangle x} \cdot \left[\mathbf{F}_{i+1}^n - \mathbf{F}_i^n\right],$$

where κ_i is the cell average of $\kappa(x)$ in the mesh cell i. The capacity function causes a change of the propagation speed of the waves. This can easily be approximated by the LTS Godunov scheme. Instead of considering the superposition of waves that are straight lines as shown in Figure 2 every wave can have a different slope in each mesh cell depending on the value of $\kappa(x_i)$. The numerical results in Figure 6 show the good performance of the LTS scheme for this problem.

The good performance of the LTS scheme for this example is not astonishing. For linear systems we would always get the most accurate approximation by applying the LTS Godunov-type scheme with a Courant number large enough that we would only need one time step to calculate the solution.

Of course we are mostly interested in solving nonlinear problems. In LeVeque [25] a truncation error analysis for nonlinear systems is given. For smooth solutions the error made during one time step due to the linear superposition is of the order $\mathcal{O}(k^3)$ which gives a contribution to the global error of order $\mathcal{O}(k^2)$, see [24] for a proof.

The projection error introduced in every time step is $\mathcal{O}(h^2)$ which gives a contribution of $\mathcal{O}(h^2/k)$ to the global error. Hence the global error of the LTS Godunov scheme is $c_1k^2 + c_2h^2/k$ with constant values c_1 and c_2. The best choice for the mesh width and time step can be obtained by setting $c_1k^2 = c_2h^2/k$ which gives a time step $k = ch^{2/3}$. Although, these analytical

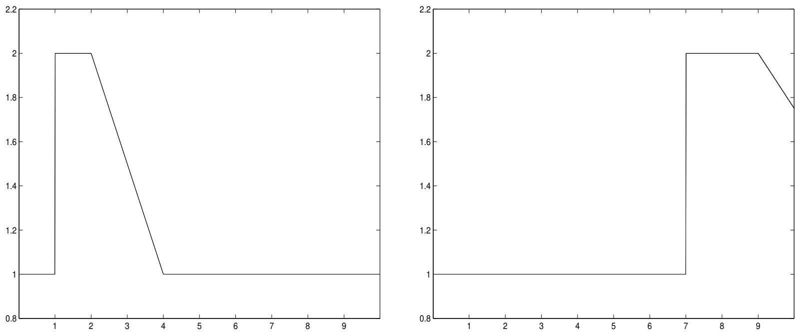

Fig. 5. Left: initial conditions, right: exact solution at time $t = 5$ for Example 2

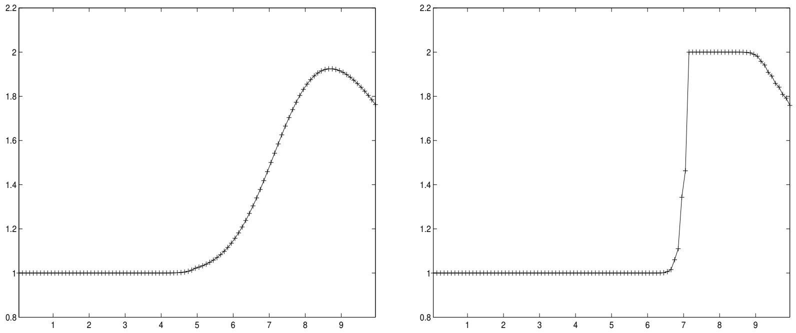

Fig. 6. Numerical solution at time $t = 5$ with $\triangle x = 0.1$ and different time steps for Example 2; Left: $CFL \leq 1$, right: $CFL \leq 10$

results are only valid for the case when h goes to zero, it indicates that we might get a more accurate solution by using time steps with Courant number larger then one at least if the solution is smooth. Numerical results confirm this. Further evidence for the advantage of using larger time steps is the error estimate of Lucier [29] for a shock-capturing scheme for scalar conservation laws of LeVeque [20], which is similar to the LTS Godunov-type scheme considered here.

5 Entropy consistency

In this section we consider the special case of a scalar conservation law with convex flux function, i.e.

$$u_t + f(u)_x = 0, \quad f^{''} > 0 \tag{9}$$

with initial values $u(x, 0) = u_0(x)$. For scalar conservation laws the LTS Godunov-type scheme converges to a weak solution in consequence of the

Lax-Wendroff Theorem and the TVD property, see LeVeque [21]. In contrast to the classical Godunov scheme with Courant number smaller or equal one, the extension for larger time steps is not monotone. This is due to the fact that the interaction of waves is considered as a linear superposition. The linear superposition of a shock and a rarefaction wave can produce values which are smaller than the minimum of the initial values.

The total variation diminishing property of the LTS scheme, which was shown in [21], guarantees that for monotone initial values the scheme is monotone. Therefore the scheme is said to be *monotonicity preserving*.

In the scalar case the solution of (9) with monotone increasing initial values consists of rarefaction waves possibly connected by constant states. Note that it is not possible that the characteristics cross each other in this case. Nevertheless, rarefaction waves from different Riemann problems can go through one and the same mesh cell which will not lead to any numerical problems. If the initial values are monotone decreasing then the solution of the scalar conservation law at a later time consists of shocks which may cross each other.

The entropy consistency for monotone schemes was proved by Harten, Hyman and Lax [9]. Hence, it follows, that the LTS Godunov scheme leads to an entropy consistent approximation as long as the initial values are monotone. This means especially that the linear superposition of arbitrary many shocks is an entropy stable approximation if h and k go to zero.

It remains to consider the interaction of shocks and rarefaction waves. First we consider the case where a rarefaction wave is moving faster then a shock as indicated in Figure 7 (a).

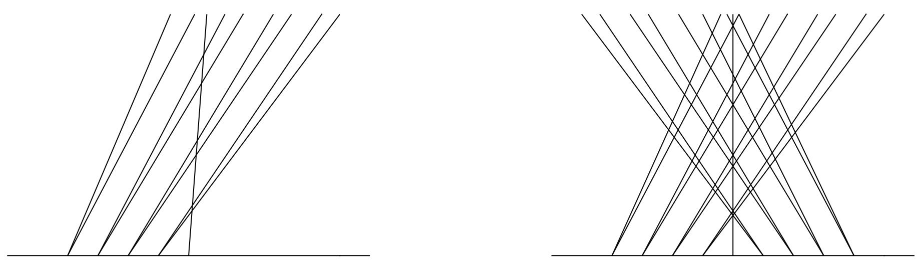

(a) $u > 0$ $u < 0$ (b) $u > 0$ $u < 0$

Fig. 7. Structure of the characteristics for two different initial values; left: interaction of rarefaction wave and shock, right: interaction of two rarefaction waves with a shock in between

As a model problem we consider Burgers equation

$$u_t + uu_x = 0$$

with initial values

$$u(x,0) = \begin{cases} 0 & : \quad x \le 1.5 \\ (x-1.5)/5.5 & : 1.5 \le x < 7 \\ -1 & : \quad x \ge 7. \end{cases}$$

The solution consists of a rarefaction wave followed by a shock which is initially located at $x = 7$ and which is then moving to the left hand side. After the first time step of the LTS scheme with a sufficiently coarse mesh, as shown in Figure 8 (left), we see that in the region to the right of the shock the value u is too small. Here we used a time step with $CFL \le 10$. If we refine the mesh and take the same Courant number this error is reduced and hardly visible, see Figure 9 (left).

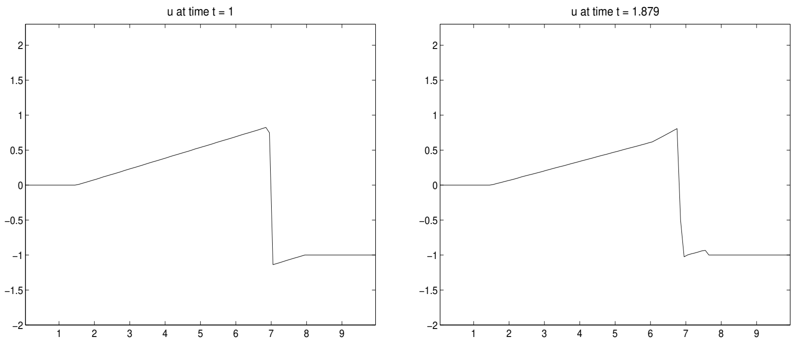

Fig. 8. Interaction of rarefaction wave and shock calculated with the LTS Godunov scheme using $\triangle x = 0.1$ and $CFL \approx 10$; Left: after first time step, right: after second time step

But also for this relatively coarse mesh the LTS Godunov scheme is correcting the error automatically by itself during the next time steps. Figure 8 (right) shows the numerical solution after the second step. Inside the region where the value of u became too small during the first time step we get a rarefaction wave which is now moving to the left hand side and which therefore corrects the error from the first time step. Also the shock is now smeared out over two mesh cells and will be approximated by one shock moving to the right and another shock moving to the left hand side. In the second time step the shock which is moving to the right creates a small region to the right of the strong shock where the solution becomes too large. An entropy violating solution to this problem can not persist because an error inside the rarefaction wave, as can be seen in Figure 8 (right), will be smeared-out in the next time step. This coincides with the motivation for the conjecture

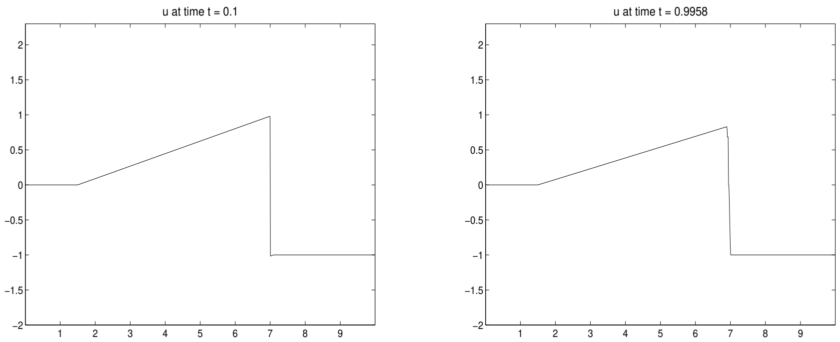

Fig. 9. Interaction of rarefaction wave and shock calculated with the LTS Godunov scheme using $\triangle x = 0.01$ and $CFL \approx 10$; Left: after first time step, right: after 10 time steps

of entropy consistency of the LTS Godunov scheme given in [21]. A similar 'self-correction' of the LTS Godunov scheme was described in LeVeque [23].

For the finer mesh we obtain a very accurate solution after ten time steps, see Figure 9 (right) which shows that the error is not accumulated for this problem. The question is whether it might be possible to construct cases where the error from one time step will increase during the next time step and where the 'self-correction' of the scheme does not work. Such a situation is considered in our next test case, where the initial values consist of two rarefaction waves which are connected by a shock.

For the numerical calculations we again consider the Burgers equation with initial values

$$u(x,0) = \begin{cases} 0 & : \quad x < 2.5 \\ 0.25(x-2.5)/2.5 & : 2.5 \leq x < 5 \\ -0.25(7.5-x)/2.5 & : 5 \leq x < 7.5 \\ 0 & : \quad x \geq 7.5. \end{cases} \tag{10}$$

For this example the shock is stationary at $x = 5$. This especially means that there is no numerical viscosity along the shock. For time steps with $CFL > 1$ the rarefaction waves from both sides of the shock cross the shock, compare with Figure 7 (b). On the left hand side of the shock the LTS Godunov-type scheme leads to values larger than the exact values and on the right hand side it leads to values which are to small. Now during the next time steps the rarefaction waves from both sides will further contribute to this error instead of smearing it out. This happens due to the symmetry of the problem. Figure 11 shows the numerical solution for $CFL \approx 20$ and different mesh widths $\triangle x$. Note that for every small perturbation of the initial values which destroys the symmetry, this structure of the numerical solution would not persist over longer times.

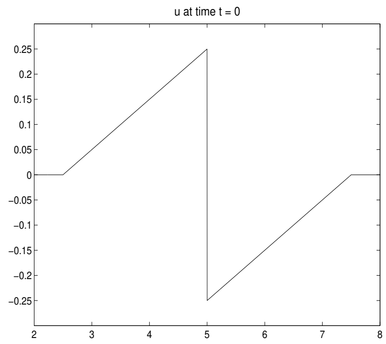

Fig. 10. Initial values as defined in Equation 10.

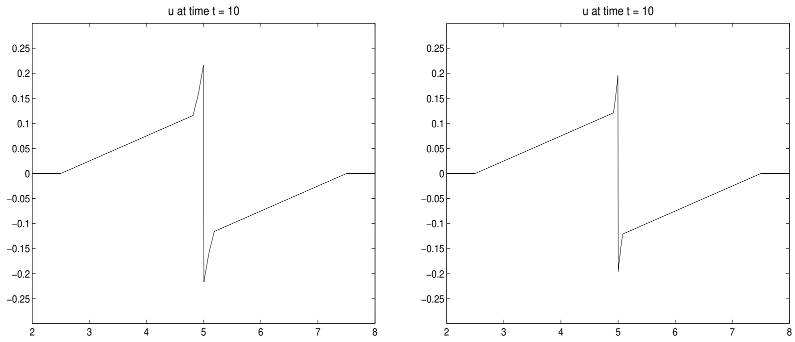

Fig. 11. Interaction of two rarefaction waves with a centred shock calculated with the LTS Godunov scheme using $CFL \leq 20$. Left: $\triangle x = 0.01$, right: $\triangle x = 0.005$

Now we want to consider the question whether the limit function would still be entropy stable. In order to do this we use Oleinik's entropy condition. It may be used for any scalar conservation law with convex flux function.

Theorem 3. *(Oleinik) Assume $d = p = 1$ and that the flux function $f : \mathbb{R} \to \mathbb{R}$ is convex. The limit function u of any sequence of approximations is the unique entropy solution of (9) if there is a constant $E > 0$ such that for all $a > 0$, $t > 0$ and $x \in \mathbb{R}$ the inequality*

$$\frac{u(x+a,t) - u(x,t)}{a} < \frac{E}{t} \tag{11}$$

is satisfied.

That equation (11) implies uniqueness is shown in Smoller [34].

The entropy condition of Oleinik has the advantage that it can be applied directly to the piecewise constant function of approximated cell averages

$u^n(x, t_n)$. In order to do this a natural choice of the parameter a would be $a = \triangle x$. A sufficient condition for the entropy consistency of the numerical scheme is that there exists a constant $E > 0$ such that

$$U_{j+1}(t) - U_j(t) < E\frac{\triangle x}{t} \tag{12}$$

for all $t > 0$ and $\triangle x \to 0$, see [26].

In Figure 12 (left) and 13 (left) we show the maximal slopes $|(U_i - U_{i-1})|/\triangle x$ occurring inside the rarefaction waves over the time t for two different discretizations with $CFL \leq 2$. For this special case the maximal discrete slope occurs between the two mesh cells to the left respectively between the two mesh cells to the right of the shock discontinuity.

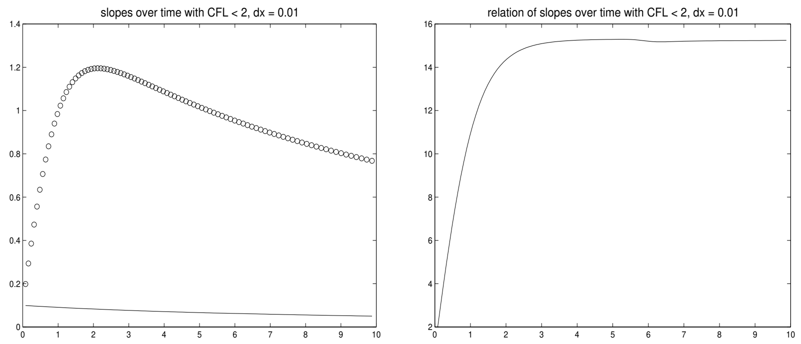

Fig. 12. Left: maximal slope (ooo) and exact slope (—) inside the rarefaction wave over time t for $\triangle x = 0.01$, $CFL \leq 2$, right: ratio between maximal slope and exact slope.

In Figure 12, 13 (left) the exact slope is also plotted, as a solid line, which is a monotone decreasing function of time. We can see that the curves of the maximal discrete slopes have a greater maximum for a finer discretization. Furthermore the function of maximal slope reaches its maximum at an earlier time if a finer mesh is used. In Figure 12 and 13 (right) we show the ratio between the maximal numerical slope and the exact slope. Here it can be seen that after this ratio has reached its maximum value the function remains constant. To explain this, we consider the cell averages in the two mesh cells to the left of the shock. These are the mesh cells $i+1$ and $i+2$ in Figure 14. The stationary shock for our example with initial values (10) sits at $x = 5$ which corresponds to the boundary between the mesh cells $i+2$ and $i+3$.

The cell average of the mesh cell $i+2$ at time t_{n+1} is equal to

$$U_{i+2}^{n+1} = U_{i+2}^n + (U_{i+1}^n - U_{i+2}^n) + A_{i+2}(U_i^n, U_{i+1}^n) + B_{i+2}(U_{i+3}^n, U_{i+4}^n).$$

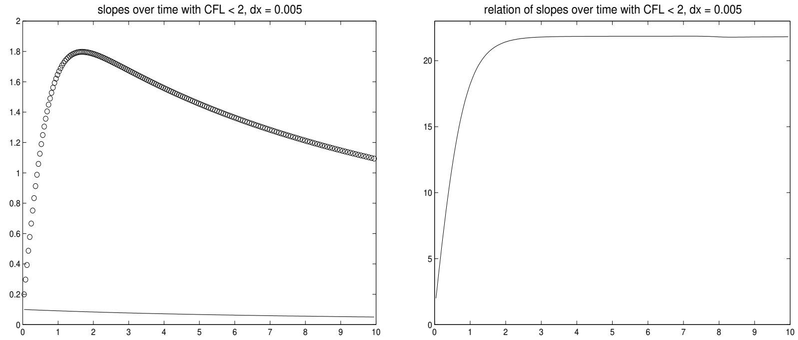

Fig. 13. Left: maximal slope inside the rarefaction wave over time t for $\triangle x = 0.005$, $CFL \leq 2$, right: ratio between maximal slope and exact slope.

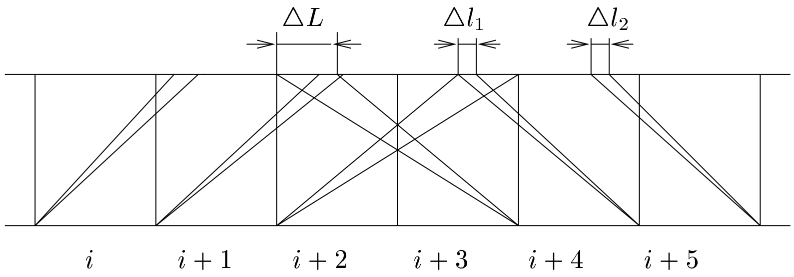

Fig. 14. Linear superposition of two rarefaction waves with an intermediate stationary shock between the mesh cells $i+2$ and $i+3$.

The term $(U_{i+1}^n - U_{i+2}^n)$ is the contribution of the rarefaction wave of the Riemann problem between the mesh cells $i+1$ and $i+2$ which completely went through the cell $i+2$. The terms $A_{i+2}(U_i^n, U_{i+1}^n)$ and $B_{i+2}(U_{i+3}^n, U_{i+4}^n)$ are the contributions of the Riemann problems between the mesh cells i and $i+1$ as well as respectively $i+3$ and $i+4$ to the value of the cell average in the mesh cell $i+2$ at time t_{n+1}. For our example the term $(U_{i+1}^n - U_{i+2}^n) + A_{i+2}(U_i^n, U_{i+1}^n)$ decreases the cell average and the term $B(U_{i+3}^n, U_{i+4}^n)$ leads to an increase of the cell average.

Note that we are taking $CFL = 2$ whereby the front of the wave originating between cells $i+3$ and $i+4$ crosses exactly two mesh cells to the left. An increase of the jump between the mesh cells $i+3$ and $i+4$ increases the wave width $\triangle L$. If the slope is relatively large compared to the slope between the other mesh cells, than also the distance $\triangle L$ becomes larger, which on the other hand has the effect that the rarefaction wave arising between mesh cell $i+3$ and $i+4$ is smeared out over a larger distance. This means that the error due to the linear superposition of the waves will again be corrected by the scheme. In contrast to the example where we only had the interaction of one rarefaction wave with a shock wave we first get an increase of the jump of the cell averages between the mesh cells $i+1$ and $i+3$ during the first time steps before the scheme will balance the error. This effect can be seen very nicely from the Figures 12 and 13 (right), which show that after some time while the jump between the two mesh cells to the left of the shock is increased, we get a balanced relation compared to the exact jump which is decreasing for our example.

For smaller mesh cells we also have smaller time steps and therefore the maximal slope will be reached earlier. The decrease of the maximal slope in Figure 12, 13 (left) is proportional to the decrease of the exact slope over time which can be seen from Figure 12, 13 (right), where we have plotted the ratio between the maximal slope inside the rarefaction waves and the exact slope.

However, as we can also see from Figure 12 and 13 the maximal slope as well as the ratio between the maximal slope and the exact slope is increasing if the mesh is refined. Therefore, we do not get an upper bound for the constant E in the discrete version of the Oleinik entropy condition (12). But we can also see that the maximal slope will not be twice as large if the mesh width is reduced by the factor two. For the special case of Burgers equation, using time steps with $CFL \leq 2$, we can show that the maximal slope will increase by a factor $\sqrt{2}$ if we bisect the mesh cells. On the other hand the region where this error occurs becomes half as large. Furthermore, we get from the TVD property of the scheme that the number of discontinuities is limited. This means that we can not get infinitely many regions where such an error might arise if we refine the mesh. Therefore, in the limit as $\triangle x$ goes to zero the error in the L_1 norm goes to zero and the solution goes to the exact solution. We can also see this from Oleinik's entropy condition if we apply it in a different form to the discrete solution. Instead of setting $a = \triangle x$ we can take the

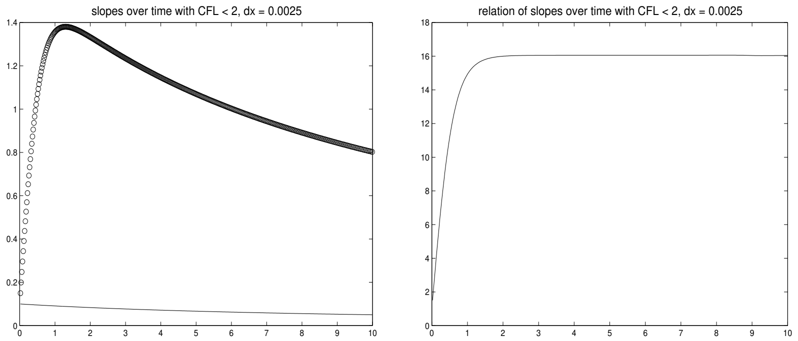

Fig. 15. Left: maximal slope for $a = 2\triangle x$ over time t with $\triangle x = 0.0025$, $CFL \leq 2$, right: ratio between this slope and the exact slope

value a arbitrary but fixed and then consider a sequence of approximations. If we for instance set $a = 0.005$ which is equal to $\triangle x$ in the calculations shown in Figure 13, then we can consider the maximal slope $|(U_{i-1} - U_i)/a|$ inside the rarefaction wave for different discretizations. Figure 15 shows the maximal slopes for this constant value of a and $\triangle x = 0.0025$. These maximal slopes can now be directly compared with those shown in Figure 13, where the same value for the constant a was used. The numerical calculations show that the slopes corresponding to the fixed value of a are decreasing as $\triangle x$ goes to zero. Therefore we have found an upper bound of the constant E to the given value a. This upper bound is equal to the maximal slope arising in the discretization with $\triangle x = a$. The case $CFL > 2$ will not lead to further problems for the example considered.

6 The LTS scheme in 2D

In this section we will restrict our considerations to two dimensional scalar conservation laws with convex flux function. The simplest way to extend the LTS Godunov scheme to two space dimensions can be obtained by using a dimension splitting approach, which was considered in LeVeque [20].

Here we want to consider another possibility, which was motivated by the 2D CLAWPACK algorithm, see [27], and is a generalization to $CFL > 1$. In contrast to the wave propagation algorithm in CLAWPACK we do not solve transverse Riemann problems, instead we consider for every mesh cell the transport due to the Riemann problems along all four cell boundaries, as will be described later.

For a 2D advection equation

$$u_t + au_x + bu_y = 0, \quad a, b > 0$$

the exact influence of a single mesh cell to the change of the cell average of the neighboring cells is indicated in Figure 16.

Here the value of the mesh cell (i, j) is shifted in x direction over a distance $a\triangle t$ and in y direction over a distance $b\triangle t$. In contrast to the dimension splitting approach we use the values u at the old time step, and not intermediate values, in order to calculate the evolution.

In order to generalize this scheme to time steps with Courant numbers larger then one, we first consider the case where the solution of the Riemann problems for both directions can be approximated by a discontinuity. This means that the solution consists either of a shock wave or of a rarefaction wave which can be approximated by a single discontinuity, i.e. no entropy-fix is necessary. The algorithm is indicated in Figure 17. If s^x_{ij} is the speed of the discontinuity for the Riemann problems between the mesh cells (i, j) and $(i + 1, j)$ then the jump across the cell interface can be propagated over a distance $s^x_{ij}\triangle t$. But we also have to take into account the propagation in y direction. Let s^y_{ij-1} and s^y_{ij} denote the speeds of the Riemann problems in y

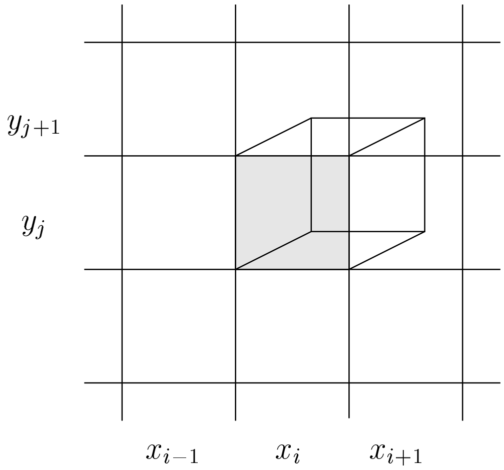

Fig. 16. Description of the flow across each cell boundary of the mesh cell (i, j) using a time step with $CFL < 1$

direction arising on the bottom and the top of the mesh cell (i, j) then the discontinuity across the mesh cells (i, j) and $(i + 1, j)$ is also propagated in y direction corresponding to these speeds. Therefore, the jump across each cell interface has an influence over a trapezoidal region as shown in Figure 17.

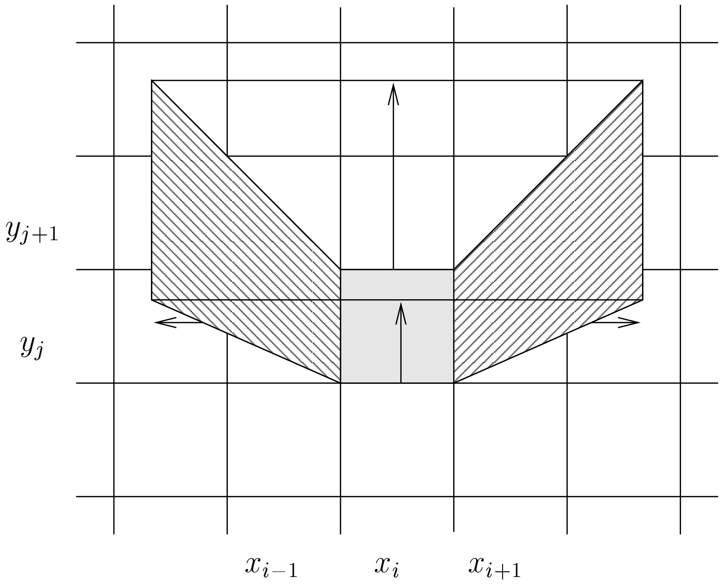

Fig. 17. Schematic description of the influence of the flow across the cell boundaries of the mesh cell (i, j) for time steps with $CFL > 1$

In order to get a conservative scheme we do not add the whole jump, for our example $u(x_{i+1}, y_j) - u(x_i, y_j)$, in the area which is covered by the trapezoid. Instead we have to normalize the jump in such a way that the change due to the Riemann problem considered is equal to

$$s^x_{ij} \triangle t \triangle y[u(x_{i+1}, y_j) - u(x_i, y_j)].$$

If we consider a cell interface where the corresponding Riemann problem in normal direction is a rarefaction wave then the trapezoidal area is divided into several trapezoids where we always have to add another cell average, corresponding to the 1D approximation of a rarefaction wave and the normalization in order to get a conservative scheme. If the Riemann problem for one or both of the transverse cell interfaces consists of a rarefaction wave then we use the most up-going part of the Riemann solution across the cell interface on the top of cell (i, j) and the most down-going part of the Riemann solution across the cell interface at the bottom to calculate the trapezoid area which is influenced by the jump across the mesh cells (i, j) and $(i + 1, j)$.

The area which is influenced by the flow over a cell interface is a trapezoid or consists of one or two triangles, depending on the waves of the transverse Riemann problems, see Figure 18 (a) and (b). In Figure 18(c) we show the reference area which is used to normalize the flux across the cell boundary considered, in order to get a conservative scheme.

In cases where the area consists of two triangles the scheme can lead to larger inaccuracies. As long as the area remains a trapezoid we expect a higher accuracy than by using the classical Godunov scheme, see Example 4

Example 4. We consider the 2D Burgers equation

$$u_t + uu_x + uu_y = 0$$

with piecewise constant initial values

$$u(x, y, 0) = \begin{cases} 1 : xy > 0 \\ 0 : xy < 0. \end{cases}$$

Along the sides of monotone deceasing initial values the solution will contain shocks and along the sides with monotone increasing initial values the solution consists of rarefaction waves. For the solution shown in Figure 19 we show the numerical results which were obtained by using our first order version of the two dimensional LTS-Godunov scheme with a time step restriction $s_{i-1,j} \triangle t \leq s_{i,j} \triangle t$ and $s_{i,j-1} \triangle t \leq s_{i,j} \triangle t$, where s is the maximal wave speed for the Riemann problem between two neighboring mesh cells either in x-direction or in y-direction. With this restriction on the time step we exclude the situation shown in Figure 18 (b), in our example this time step restriction corresponds to a Courant number slightly smaller than two. We compare our solution with those obtained by using the first order version of CLAWPACK, see Figure 20. One clearly sees that the larger Courant number leads to less smearing of the solution.

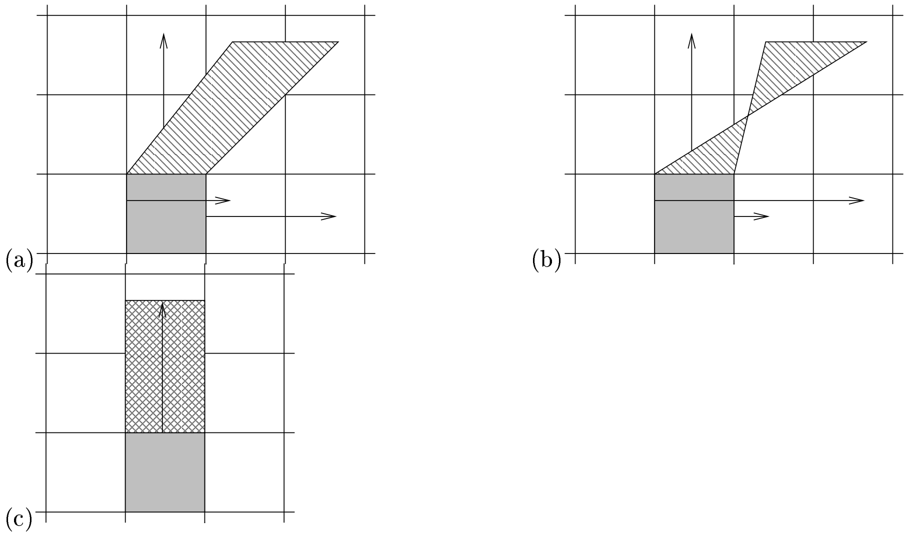

Fig. 18. Different possibilities for the area that is influenced by a Riemann problem in y-direction

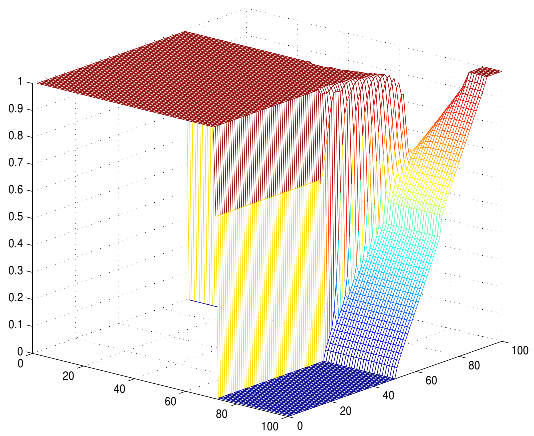

Fig. 19. Solution of Example 4 at time $t = 40$ with $\triangle x = 1$ using the LTS Godunov scheme

Conclusions and outlook

The article reviewed the current state of development of the large time step scheme of LeVeque for hyperbolic conservation laws. A key open problem for over a decade was the entropy consistency, even for scalar conservation laws with convex flux function, for Courant numbers larger then two. The key

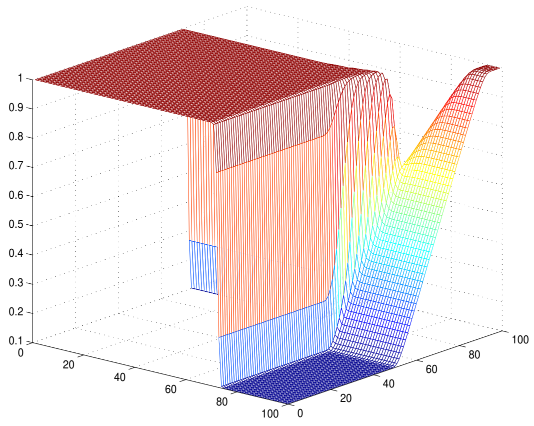

Fig. 20. Solution of Example 4 at time $t = 40$ with $\triangle x = 1$ using the first order CLAWPACK algorithm with $CFL \leq 1$

difficulty in proving this is the interaction of shocks with rarefaction waves. We presented some numerical experiments that should be helpful in order to prove the entropy-consistency of the scheme.

The advantage of using Courant numbers larger than one in finite volume schemes lies not only in the fact that fewer time steps are needed to cover a given time interval. There is also a reduction of the numerical dissipation and corresponding gain in accuracy for at least moderately higher Courant numbers. Also, in general flows there are frequently large regions where the nonlinearities are very weak, so that these schemes can be accurate at least locally for quite large Courant numbers.

Though we present an improvement for scalar multidimensional conservation laws, the extension to multidimensional systems is what is really needed in the future. This would be of considerable interest to the computational fluid dynamics community, even if these type of schemes were used only locally in adaptive calculations.

Acknowledgments This work was supported by the DFG Priority Program DANSE. We would like to thank Professor Bernold Fiedler for the coordination of this program.

References

1. S.J. Billett and E.F. Toro: On WAF-type schemes for multidimensional hyperbolic conservation laws. J. Comput. Phys. **130** (1997) 1-24.

2. A.J. Chorin: Random choice solution of hyperbolic systems. J. Comput. Phys. **22** (1976) 517-533.
3. R. Courant and K.O. Friedrichs and H. Lewy: Über die partiellen Differenzengleichungen der mathematischen Physik. Math. Ann. **100** (1928) 32-74.
4. E. Godlewski and P.-A. Raviart: Hyperbolic Systems of Conservation Laws. Ellipses, 1990.
5. E. Godlewski and P.-A. Raviart: Numerical Approximation of Hyperbolic Systems of Conservation Laws. Springer-Verlag, 1995.
6. S.K. Godunov: A difference scheme for numerical computation of discontinuous solutions of equations of fluid dynamics. Mat. Sb. **47** (1959) 271-306.
7. E. Hairer: Unconditionally stable explicit methods for parabolic equations. Numer. Math. **35** (1980) 57-68.
8. A. Harten and J.M. Hyman: Self adjusting grid methods for one-dimensional hyperbolic conservation laws. J. Comp. Phys. **50** (1983) 235-269.
9. A. Harten and J.M. Hyman and P.D. Lax: On finite difference approximations and entropy conditions for shocks. Comm. Pure Appl. Math. **29** (1976) 297-322.
10. A. Harten and P.D. Lax: A random choice finite difference scheme for hyperbolic conservation laws. SIAM J. Numer. Anal. **18** (1981) 289-315.
11. A. Harten and P.D. Lax and B. van Leer: On upstream differencing and Godunov-type schemes for hyperbolic conservation laws. SIAM Review **25** (1983) 35-61.
12. H. Holden and K.-A. Lie and N.H. Risebro: An unconditionally stable method for the Euler equations. J. Comput. Phys. **150** (1999) 76-96.
13. H. Holden and N.H. Risebro: A method of fractional steps for scalar conservation laws without the CFL condition. Math. of Comp. **60** (1993) 221-232.
14. U. Iben and E. Tadmor: High resolution schemes for conservation laws in the simulation of injection systems. Technical Report 00-06, UCLA, 2000.
15. R. Klein: Semi-implicit extension of a Godunov-type scheme based on low Mach number asymptotics I: One-dimensional flow. J. Comput. Phys. **121** (1995) 213-237.
16. D. Kröner: Numerical Schemes for Conservation Laws. Teubner-Verlag, 1997.
17. P.D. Lax and B. Wendroff: Systems of conservation laws. Comm. Pure Appl. Math. **13** (1960) 217-237.
18. R.J. LeVeque: CLAWPACK software. available from `http://www.amath.washington.edu/~rjl/clawpack.html`
19. R.J. LeVeque: CLAWPACK User Notes.
20. R.J. LeVeque: Large time step shock-capturing techniques for scalar conservation laws. SIAM J. Numer. Anal. **19** (1982) 1091-1109.
21. R.J. LeVeque: Convergence of a large time step generalization of Godunov's method. Comm. Pure Appl. Math. **37** (1984) 463-477.
22. R.J. LeVeque: A large time step generalization of Godunov's method for systems of conservation laws. SIAM J. Numer. Anal. **22** (1985) 1051-1073.
23. R.J. LeVeque: Some preliminary results using a large time step generalization of the Godunov method. In F. Angrand et. al, editors, Numerical methods for the Euler equations of Fluid Dynamics, SIAM, Philadelphia (1985) 32-47.
24. R.J. LeVeque: Second order accuracy of Brenier's time-discrete method for nonlinear systems of conservation laws. SIAM J. Numer. Anal. **25** (1988) 1-7.
25. R.J. LeVeque: Hyperbolic conservation laws and numerical methods. Von Karman Institute of Fluid Dynamics Lecture Series, 90-3, 1990

26. R.J. LeVeque: Numerical Methods for Conservation Laws. Birkhäuser Verlag, 1990.
27. R.J. LeVeque: Wave propagation algorithms for multidimensional hyperbolic systems. J. Comput. Phys. **131** (1997) 327-353.
28. R.J. LeVeque: Nonlinear Conservation Laws and Finite Volume Methods for Astrophysical Fluid Flow. In O. Steiner and A. Gautschy, editors, Computational Method for Astrophysical Fluid Flow, 27th Saas-Fee advanced course lecture note, Springer-Verlag, 1998.
29. B.J. Lucier: Error bounds for the methods of Glimm, Godunov and LeVeque. SIAM J. Numer. Anal. **22** (1985) 1074-1081.
30. K.W. Morton: On the analysis of finite volume methods for evolutionary problems. SIAM J. Numer. Anal. **35** (1998) 2195-2222.
31. P.L. Roe: Approximate Riemann solver, parameter vectors, and difference schemes. J. Comput. Phys. **43** (1981) 357-372.
32. N. Satofuka: A new explicit method for the numerical solution of parabolic differential equations. Numerical properties and methodologies in heat transfer, Proc. 2nd nat. Symp., College Park, 1981, 97-108, 1983.
33. N. Satofuka: Numerical solution of fluid dynamic equations using rational Runge-Kutta methods. Comp. Meth. in Appl. Sci. Eng. **VII** (1986) 249-259.
34. J. Smoller: Shock Waves and Reaction-Diffusion Equations. Springer-Verlag, 1994.
35. E.F. Toro: Riemann solvers and numerical methods for fluid dynamics. Springer-Verlag, 1997.
36. E.F. Toro and S.J. Billett: A unified Riemann-problem-based extension of the Warming-Beam and Lax-Wendroff schemes. IMA J. Numer. Anal. **17** (1997) 61-102.
37. J. Wang: Large time step generalizations of Glimm's scheme for systems of conservation laws. Chin. Ann. of Math. **913** (1988) 50-63.
38. J. Wang and G. Warnecke: On entropy consistency of large time step schemes I. The Godunov and Glimm schemes. SIAM J. Numer. Anal. **30** (1993) 1229-1251.
39. J. Wang and G. Warnecke: On entropy consistency of large time step schemes II. Approximate Riemann solvers. SIAM J. Numer. Anal. **30** (1993) 1252-1267.